

Dissociation of Single-Strand DNA: Single-Walled Carbon Nanotube Hybrids by Watson–Crick Base-Pairing

Seungwon Jung,[†] Misun Cha,^{*,‡} Jiyong Park,^{§,#} Namjo Jeong,^{†,||} Gunn Kim,^{§,¶} Changwon Park,[§] Jisoon Ihm,[§] and Junghoon Lee^{*,†,‡}

School of Mechanical and Aerospace Engineering, Seoul National University, Seoul 151-742, Korea, Institute of Advanced Machinery and Design, Seoul National University, Seoul 151-744, Korea, FPRD and Department of Physics and Astronomy, Seoul National University, Seoul 151-742, Korea, and Nanomaterials Research Center, Korea Institute of Energy Research, Daejeon 305-343, Korea

Received March 30, 2010; E-mail: jleenano@snu.ac.kr; cmsbest@snu.ac.kr

Abstract: It has been known that single-strand DNA wraps around a single-walled carbon nanotube (SWNT) by π -stacking. In this paper it is demonstrated that such DNA is dissociated from the SWNT by Watson–Crick base-pairing with a complementary sequence. Measurement of field effect transistor characteristics indicates a shift of the electrical properties as a result of this “unwrapping” event. We further confirm the suggested process through Raman spectroscopy and gel electrophoresis. Experimental results are verified in view of atomistic mechanisms with molecular dynamics simulations and binding energy analyses.

Single-strand DNA (ssDNA) forms a hybrid with a single-walled carbon nanotube (SWNT) through π -stacking between the bases of the ssDNA and the atomic structures on the sidewall of the SWNT.^{1,2} The ssDNA–SWNT hybrid has gained interest as a new nano–bio conjugate for various applications such as drug delivery,³ biochemical sensors,^{4–6} and the sorting of SWNTs.^{7,8} It has also been revealed that the optical and electrical properties of the SWNT may be altered by the interaction between the ssDNA and the SWNT.^{9–11}

A next step in exploring the significance of this interaction would be to consider an aftermath of Watson–Crick base-pairing or hybridization by introducing a DNA sequence complementary to the ssDNA attached on the SWNT. Hybridization has been confirmed by electrochemical and optical methods such as the shift of field effect transistor (FET) characteristics⁵ and band gap fluorescence modulation,⁶ while the reaction with non-complementary DNA resulted in no change, as predicted.^{5,6,12} However, the detailed mechanism and the consequences of the hybridization are still controversial. Some papers suggest that the double-strand DNA (dsDNA) will remain attached along the aromatic group on the sidewall of the SWNT after base-pairing.^{5,6} Others favor desorption from the sidewall of the SWNT as the dsDNA is formed.^{12,13}

In this paper, we report experimental and theoretical proofs that unambiguously support the detachment of the hybridized dsDNA from the SWNT. This wrapping–unwrapping transition is primarily evidenced by a shift of electrical properties, monitored through an FET-type measurement. As previously reported, a metallic SWNT,

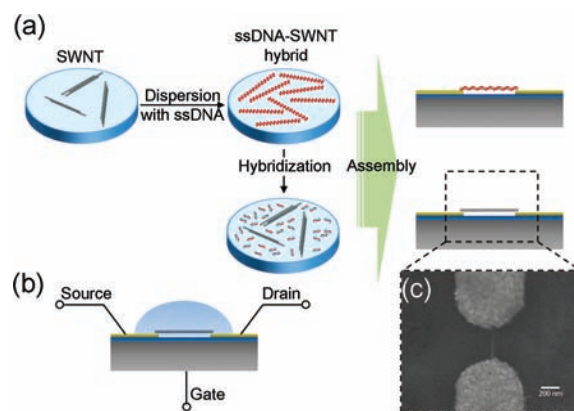


Figure 1. Schematic of monitoring DNA hybridization. (a) Procedure of the DNA hybridization experiment. (b) Schematic of the FET measurement. (c) Scanning electron microscopy (SEM) image of the assembled SWNT.

when forming a hybrid with an ssDNA, shows p-type semiconducting behavior.¹¹ Here we demonstrate that the electrical property of the hybridized product essentially returns to the metallic state as a result of the unwrapping event. This unwrapping process is also confirmed through gel electrophoresis and further verified with Raman spectroscopy. We also use molecular dynamics (MD) simulations and binding energy analyses to study the mechanisms in detail.

Figure 1 shows a schematic of the experimental procedure and the FET measurement. Initially, 0.1 mg of SWNTs synthesized through the high-pressure carbon monoxide conversion process (HiPco, Carbon Nanotechnologies, Inc., Houston, TX) was dispersed with 10 μ M ssDNAs by using sonication and centrifugation in deionized (DI) water.¹¹ Since there was an excess amount of SWNTs, the ssDNAs were completely consumed by forming hybrids that were well dispersed in water. The unbound SWNTs were removed by centrifugation. Our observation with a spectrophotometer (NANODROP 2000, Thermo Fisher Scientific Inc., Waltham, MA) indicates that the ssDNAs were completely consumed during the formation of the ssDNA–SWNT hybrids (see the Supporting Information). The resulting solution with the ssDNA–SWNT hybrids was diluted by 10 times with DI water, followed by the hybridization process in which 1 μ M complementary DNAs (cDNAs) were injected into the ssDNA–SWNT hybrid solution. The hybridization was carried out in a buffer solution (50 mM phosphate-buffered saline, equivalently mixed during the hybridization) to improve the efficiency.¹⁴

The sample after the reaction was dielectrophoretically (at 5 MHz and 5 V for 1 min) deposited between the electrodes with 300 nm

[†] School of Mechanical and Aerospace Engineering, Seoul National University.

[‡] Institute of Advanced Machinery and Design, Seoul National University.

[§] FPRD and Department of Physics and Astronomy, Seoul National University.

^{||} Nanomaterials Research Center, Korea Institute of Energy Research.

[¶] Current address: Department of Physics, Kyung Hee University, Seoul 130-701, Korea.

[#] Current address: Howard Hughes Medical Institute and UCLA-DOE Institute for Genomics and Proteomics, Los Angeles, California 90095-1570.

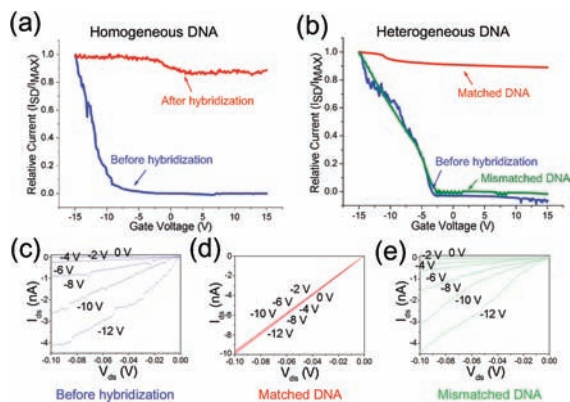


Figure 2. Results of hybridization: (a) $I_{ds}-V_G$ for matched homogeneous sequence; (b) $I_{ds}-V_G$ for matched and mismatched heterogeneous cases; (c–e) $I_{ds}-V_{ds}$ for heterogeneous cases in (b).

gap in 30 pairs which were prefabricated through nanoimprint lithography (NIL).¹¹ The dielectrophoretic alignment and assembly under the given conditions resulted in predominantly metallic SWNTs captured and deposited, even when the SWNTs were wrapped with DNAs.^{15,16} FET measurement was done to obtain a source-drain current by sweeping the gate voltage from -15 to $+15$ V at a constant source-drain bias voltage of 100 mV.¹⁷

Figure 2 shows the electrical properties of the ssDNA–SWNT hybrids measured before and after hybridization. The hybridization experiment in Figure 2a used a homogeneous sequence: 18-mer poly(C)–SWNT hybrid and poly(G) target with the same length. The signal was normalized by the maximum value of the measured current (raw graphs and hysteresis are included in Supporting Information). It has been previously reported that the electronic structure of the metallic SWNT was significantly affected by the helical wrapping of the ssDNA, resulting in the semiconducting behavior¹¹ indicated in Figure 2. This semiconducting property of the ssDNA-decorated metallic SWNTs was the result of electron transfer from the SWNT to the ssDNA. Water molecules were found critical to activate this metal–semiconductor transition in the ssDNA–SWNT hybrid. Thus, every reaction and measurement in this paper were carried out in a wet state. As a result of the hybridization with cDNA, the current response of the SWNT shifted upward and became almost flat, reclaiming the original metallic characteristic. A similar outcome was observed when a heterogeneous sequence was used (Figure 2b). The sequence used in this case (target DNA: 5′-cga ccg acg tcg gtc gg-3′) has been selected for the detection of human papillomavirus (HPV).¹⁸ These results show that the shift of the conducting property resulting from the interaction of DNA is essentially sequence-independent. On the contrary, such a shift was not observed when the mismatched sequence (5′-tcc gac cga cgt cgg tt-3′) was introduced, indicating no interaction between the hybrid and the control. This result is consistent with previous studies.^{5,6,12}

In Figure 3a, gel electrophoresis (15% polyacrylamide gel) reveals the fate of the dsDNA released as a result of the hybridization. Ethidium bromide (EtBr) dye embedded in the polyacrylamide gel would stain dsDNA as a result of intercalation. Lane 1, loaded with the ssDNA–SWNT hybrid, shows no such staining because the ssDNA is firmly attached to the SWNT. Lane 2 shows a weak signal due to the nonspecific self-conformation of the ssDNA. Lane 3 was loaded with the dsDNA obtained by hybridization as a control, resulting in strong fluorescence. Lane 4 was loaded with the product of the reaction of ssDNA–SWNT hybrid and the complementary sequence. The fluorescence band in lane 4 coincides with that of the control in lane 3, which manifests

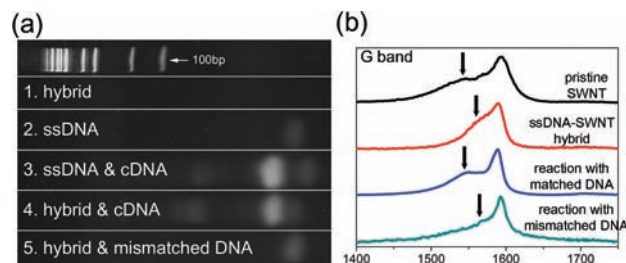


Figure 3. Experimental evidence for unwrapping due to hybridization: (a) gel electrophoresis and (b) tangential bands (G-bands) in Raman spectra.

the hybridization and unwrapping. The weak bands in lanes 3 and 4 indicate residual cDNA added as surplus. Lane 5, loaded with the product of the reaction of ssDNA–SWNT hybrid and the mismatched sequence, clearly shows the lack of the strong band.

Raman spectroscopy was used to further investigate the unwrapping event due to the hybridization. Radial breathing modes (RBMs) and tangential modes (G-bands) were measured for the pristine SWNT and the ssDNA–SWNT hybrids in water before and after the hybridization. A micro-Raman system (LabRam HR, Jobin-Yvon, Longjumeau, France) was used with laser lines at a wavelength of 514.5 nm from an Ar ion laser. The diameter of the SWNT used in this study was determined by analysis of the RBM peaks¹⁹ (RBM peaks are described in Supporting Information) as 1.1 ± 0.2 nm for all three cases. The G-bands in Figure 3b show a noticeable difference between the states before and after hybridization. The pristine SWNT shows a broad and asymmetric Breit–Wigner–Fano (BWF) line shape (vertical arrow in Figure 3b) unique to the Raman spectra of metallic SWNTs.²⁰ The BWF line of the ssDNA–SWNT hybrids in solution was shifted to higher frequency, which agrees with previous results.¹¹ After hybridization with the cDNA, however, the BWF line clearly shifted back to a lower frequency that corresponds to the metallic property regained by unwrapping.

To understand the atomistic mechanism of the ssDNA–SWNT hybrid formation and the DNA hybridization reaction observed in our experiment, we carried out MD simulations and subsequent binding energy analyses. We identified several states of interest whose energy differences drive the overall progress of the chemical reactions observed in our experiments (Figure 4a). The binding energy was approximated as the sum of vacuum, polar, and nonpolar solvation free energies as well as trans-rotational and vibrational entropic contributions.²¹ A copy of ssDNA (5′-ccg acc gac gtc ggt cg-3′) initially wrapped around an (8,8) armchair-type SWNT, and its cDNA (5′-cga ccg acg tcg gtc gg-3′) was solvated in medium. The nucleic acid base of ssDNA made tight contact with the SWNT; the average distance from the SWNT to nucleic acid base atoms of DNA was 0.43 nm, and the distribution of the distances peaked sharply around its mean (Figure 4b). The backbone phosphate atom of ssDNA was 0.58 nm away from the SWNT. This indicates that the base atoms made tight contact with the SWNT, since the van der Waals radii of the carbon (phosphate) atoms are 0.2 (0.21) nm, and thus the adsorption of ssDNA was mediated by the base-to-SWNT interaction. These findings are in good agreement with our experimental result. As the two ssDNAs constructed a dsDNA on the SWNT surface, energy (134 kcal/mol) was released (an exothermic process).

After the hybridization, the dsDNA could be detached from the SWNT because of the weaker binding energy. The surface groove of the dsDNA may still make contact with the SWNT;²² however, the contact became less intact relative to the ssDNA–SWNT complex. Before the hybridization, the number of atomic contacts

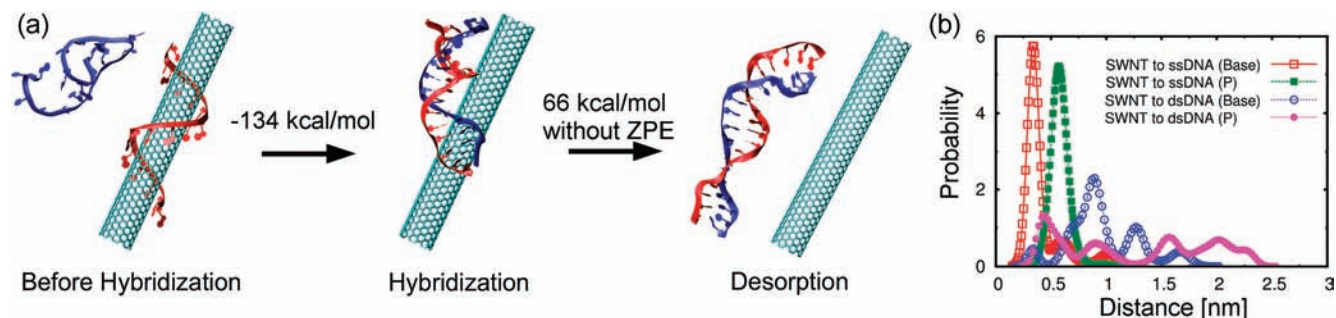


Figure 4. Energy change and detachment of dsDNA associated with the hybridization reaction. (a) Binding energy differences between relatively stable states. (b) The distance from the SWNT surface to base and phosphate (P) atoms in DNA molecules adsorbed on the SWNT surface.

between the ssDNA and the SWNT was 527, while it became 114 after the hybridization. The distance from the SWNT to the phosphate atoms of the dsDNA was 1.25 nm, and the distribution became dispersed after the hybridization reaction (Figure 4b). In addition, dsDNA diffused more freely on the SWNT surface than the ssDNA; the root-mean-squared deviation (rmsd) of the ssDNA along the SWNT axis throughout the last 5 ns of the MD simulation trajectory was 5.87 Å, whereas it was 8.10 Å for the case of dsDNA on the SWNT after the hybridization. On the other hand, 66 kcal/mol was needed to detach the dsDNA from the SWNT surface according to the method described at the end (without zero-point energy correction). If we include the zero-point energy correction, this number would be reduced to ~40 kcal/mol. In addition, the hybridized dsDNA would be vulnerable to external perturbations such as agitation and heating (which could happen during the hybridization process in general) and could easily be detached from the SWNT. On the basis of these observations, we conclude that spontaneous desorption of some dsDNAs from the SWNT surface was likely to occur following the Watson–Crick base-pairing between ssDNAs. To recapitulate, the hybridization and subsequent detachment of the dsDNA were key steps for the recovery of the metallic characteristics, as they could substantially reduce the electron transfer from the adsorbed ssDNA to the SWNT.

In summary, the unwrapping of ssDNA from the SWNT during Watson–Crick base-pairing was confirmed through electrical and optical methods and binding energy calculations. While the ssDNA–metallic SWNT hybrid showed a p-type semiconducting property, the hybridization product recovered metallic properties. Gel electrophoresis directly verified the results of wrapping and unwrapping events, which was also reflected in the Raman shifts. The MD simulations and binding energy calculations provided an atomistic description of the pathway for this phenomenon. This nano–physical phenomenon will open up a new approach for nano–bio sensing of specific sequences with the advantages of efficient particle-based recognition, no labeling, and direct electrical detection which can be easily realized in a microfluidic chip format.

Acknowledgment. We thank M. K. Choi in Raman Research Center for fruitful discussion. The experimental parts of this work were supported by the Pioneer R&D Program for Converging Technology (Grant No. M10711270001-08M1127-00110) and the WCU (World Class University) Program (Grant No. R31-2008-000-10083-0) (J.L.). The theoretical parts of this work were supported by the Center for Nanotubes and Nanostructured Composites (C.P. and J.I.). All the programs above were administered by the National Research Foundation (NRF), and funded

by the Ministry of Education, Science and Technology (MEST) of Korea. Fabrication and experiments were performed at the Inter-university Semiconductor Research Center (ISRC) in Seoul National University. The computations were performed through the support of the Korean Institute of Science and Technology Information (KISTI).

Supporting Information Available: Detailed experimental and MD simulation methods, raw data of the FET measurements, and AFM and TEM images. This material is available free of charge via the Internet at <http://pubs.acs.org>.

References

- Zheng, M.; Jagota, A.; Semke, E. D.; Diner, B. A.; Mclean, R. S.; Lustig, S. R.; Richardson, R. E.; Tassi, N. G. *Nat. Mater.* **2003**, *2*, 338–342.
- Zheng, M.; Jagota, A.; Strano, M. S.; Santos, A. P.; Barone, P.; Chou, S. G.; Diner, B. A.; Dresselhaus, M. S.; Mclean, R. S.; Onoa, G. B.; Samsonidze, G. G.; Semke, E. D.; Usrey, M.; Walls, D. *J. Science* **2003**, *302*, 1545–1548.
- Kam, N. W. S.; O'Connell, M.; Wisdom, J. A.; Dai, H. *Proc. Natl. Acad. Sci. U.S.A.* **2005**, *102*, 11600–11605.
- Staii, C.; Chen, M.; Gelperin, A.; Johnson, A. T., Jr. *Nano Lett.* **2005**, *5*, 1774–1778.
- Star, A.; Tu, E.; Niemann, J.; Gabriel, J.-C. P.; Joiner, S.; Valcke, C. *Proc. Natl. Acad. Sci. U.S.A.* **2006**, *103*, 921–926.
- Jeng, E. S.; Moll, A. E.; Roy, A. C.; Gastala, J. B.; Strano, M. S. *Nano Lett.* **2006**, *6*, 371–375.
- Tu, X.; Manohar, S.; Jagota, A.; Zheng, M. *Nature* **2009**, *460*, 250–253.
- Hersam, M. C. *Nat. Nanotechnol.* **2008**, *3*, 387–394.
- Heller, D. A.; Jeng, E. S.; Yeung, T.-K.; Martinez, B. M.; Moll, A. E.; Gastala, J. B.; Strano, M. S. *Science* **2006**, *311*, 508–511.
- Kawamoto, H.; Uchida, T.; Kojima, K.; Tachibana, M. *J. Appl. Phys.* **2006**, *99*, 094309.
- Cha, M.; Jung, S.; Cha, M.-H.; Kim, G.; Ihm, J.; Lee, J. *Nano Lett.* **2009**, *9*, 1345–1349.
- Chen, R. J.; Zhang, Y. *J. Phys. Chem. B* **2006**, *110*, 54–57.
- Karachevtsev, V. A.; Gladchenko, G. O.; Karachevtsev, M. V.; Glamazda, A. Y.; Leontiev, V. S.; Lytvyn, O. S.; Dettlaff-Weglikowska, U. *Mol. Cryst. Liq. Cryst.* **2008**, *497*, 339–351.
- Sambrooke, J.; Russel, D. W. *Molecular Cloning: A Laboratory Manual*, 3rd ed.; Cold Spring Harbor Laboratory Press: New York, 2001; Chapter 10.
- Krupke, R.; Hennrich, F.; Löhneysen, H.; Kappes, M. M. *Science* **2003**, *301*, 344–347.
- Sickert, D.; Taegar, S.; Neumann, A.; Jost, O.; Eckstein, G.; Mertig, M.; Pompe, W. *AIP Conf. Proc.* **2005**, *786*, 271–274.
- Kim, W.; Javey, A.; Vermesh, O.; Wang, Q.; Li, Y.; Dai, H. *Nano Lett.* **2003**, *3*, 193–198.
- Rashmi, S. H.; Steven, R. G.; Laimonis, A. L.; Paul, B. S. *Nature* **1992**, *359*, 505–512.
- Saito, R.; Takeya, T.; Kimura, T.; Dresselhaus, G.; Dresselhaus, M. S. *Phys. Rev. B* **1998**, *57*, 4145–4153.
- Brown, S. D. M.; Jorio, A.; Corio, P.; Dresselhaus, M. S.; Dresselhaus, G.; Saito, R.; Kneipp, K. *Phys. Rev. B* **2001**, *63*, 155414–155421.
- Wang, W.; Kollman, P. A. *J. Mol. Biol.* **2000**, *303*, 567–582.
- Zhao, X.; Johnson, J. K. *J. Am. Chem. Soc.* **2007**, *129*, 10438–10445.
- Chi, Q.; Göpel, W.; Ruzgas, T.; Gorton, L.; Heiduschka, P. *Electroanalysis* **2005**, *9*, 357–365.

JA102673M